nuclear fusion
IAEA

PAPER

The role of edge plasma parameters in H-mode density limit on the JET-ILW

To cite this article: H.J. Sun *et al* 2021 *Nucl. Fusion* **61** 066009

IOP Publishing | International Atomic Energy Agency Nuclear Fusion

Nucl. Fusion **61** (2021) 066009 (7pp) https://doi.org/10.1088/1741-4326/abf056

The role of edge plasma parameters in H-mode density limit on the JET-ILW

H.J. Sun[1], R.J. Goldston[2], A. Huber[3], X.Q. Xu[4], J. Flanagan[1], D.C. McDonald[1], E. de la Luna[5], M. Maslov[1], J.R. Harrison[1], F. Militello[1], J. Fessey[1], S. Cramp[1] and JET Contributors[a]

[1] UKAEA/CCFE, Culham Science Centre, Abingdon, Oxon, OX14 3DB, United Kingdom of Great Britain and Northern Ireland
[2] Princeton Plasma Physics Laboratory, Princeton, United States of America
[3] Forschungszentrum Jülich, Institut für Energie- und Klimaforschung—Plasmaphysik, 52425 Jülich, Germany
[4] Lawrence Livermore National Laboratory, Livermore, United States of America
[5] Laboratorio Nacional de Fusión, Asociación EURATOM-CIEMAT, Madrid, Spain

E-mail: HongJuan.SUN@UKAEA.UK

Received 2 February 2021, revised 7 March 2021
Accepted for publication 19 March 2021
Published 28 April 2021

Abstract

A study of a dataset of JET H-mode plasma with the Be/W ITER-like wall (JET-ILW) shows that reaching the edge MHD ballooning limit leads to confinement degradation. However, unlike JET plasmas with a carbon wall (JET-C), the JET-ILW plasmas stay in a marginal dithering phase for a relatively long period, associated with a higher (≈20%) H-mode density limit (HDL) than JET-C equivalents. This suggests that ITER could be operated in H-mode with higher density than the scaling based on carbon wall devices, but likely with a dithering phase plasma with lower confinement. A new, reliable estimator for JET $E_{r,\,min}$ has been derived by combining HRTS measurements of pedestal gradient and edge-SOL decay lengths. JET radial E_r ETB wells are observed in the range of -15 to -60 kV m^{-1} in high performance H-modes, consistent with previous CXRS results in ASDEX Upgrade. The results imply that a higher positive $E \times B$ shear in the near SOL plays a role in sustaining a marginal phase in JET-ILW which leads to a higher HDL than that in JET-C. The results of the JET-ILW dataset show agreement with the Goldston finite collisionality HD model for SOL broadening at high collisionality. A hypothesis for the dithering H-mode phase is proposed: as $n_{e,SOL}$ increases, $\nu_{*,SOL}$ increases, SOL broadens, E_r shear decreases, triggers L-mode; n_e drops, $\nu_{*,SOL}$ decreases, SOL becomes narrower, and E_r shear increases, triggering H-mode, resulting in a cycle of H–L–H- oscillations. For burning plasma devices, such as ITER, operating just below the MHD limit for the dithering phase could be a promising regime for maximising core density, and fusion performance while minimising plasma-material interaction. The oscillatory signal during the dithering phase could be used as a precursor of undesirable plasma performance for control purposes.

Keywords: JET-ILW, H-mode density limit, edge ballooning limit, radial electrical field, SOL decay length

(Some figures may appear in colour only in the online journal)

* Author to whom any correspondence should be addressed.
[a] See Joffrin et al 2019 (https://doi.org/10.1088/1741-4326/ab2276) for the JET Team.

1. Introduction

It is desirable to run future experiments and power plants at the highest plasma densities possible to increase their performance and reduce the power reaching the targets. For the optimal temperature, increased plasma density leads to a significant increase of the fusion power for future machines since the fusion reaction rate scales with n^2 [1]. The present solution for handling the heat load on the divertor in ITER is to radiate a significant amount of power in the plasma edge and divertor to minimize the power flow directly to the divertor targets [2]. This requires burning plasma devices, such as ITER, to operate at high density to enable partial or total divertor detachment [2]. However, the highest density at which stable plasma can be produced in tokamaks is always found to be limited. Through empirical study of a large set of plasma on multiple tokamaks, the Greenwald density limit has been derived to describe this limit [3, 4]. It is found to depend on plasma current and machine size. When the Greenwald density is reached, the plasma is likely ended with disruption. Furthermore, the high confinement plasma (H-mode) cannot be sustained when the density approaches the Greenwald limit, which puts an extra limitation on the highest operational density [5]. This so-called H-mode density limit (HDL) is a soft limit, as it is a back transition to L-mode at high densities and the plasma operation can be continued with a lower confinement.

Since H-mode at high density is the foreseen promising operational regime for ITER and other future fusion devices [6, 7], dedicated studies have been performed in various machines to investigate underlying physics on HDL and to seek the methods to expand the operational place [8–15]. Recent studies on ASDEX Upgrade (AUG) and the Joint European Torus (JET) show that the total radiated power stay constant for a period before reaching the HDL. On both AUG and JET, HDL can occur without the formation of an MARFE (multifaceted asymmetric radiation from the edge [16]) and H-mode plasma can be sustained under completely divertor detached conditions. Thus, excessive radiation, MARFE and divertor detachment, which were considered as candidates for HDL in earlier studies for HDL, have been ruled out as a cause of the final trigger of the H–L back transition [11, 12].

With centrally elevated density profiles, e.g. by pellet fuelling, it is possible to exceed the HDL and even the Greenwald limit at a reasonable H-mode confinement [10, 11]. However, the exceedance of the Greenwald density limit for H-modes features largely elevated core density profiles but low edge densities. This is strong evidence that both limits are determined by the plasma parameters at the pedestal top and further outside. The divertor configuration has an obvious impact in HDL [12]. The HDL in JET with vertical target configurations is about 15%–18% lower than the HDL plasma with outer strike point on the horizontal target. At high density, JET plasma with a Be/W ITER-like wall (JET-ILW) always enters a dithering phase before the H–L back transition, which enables a (≈20%) higher HDL than in JET-C. The impact of the divertor configuration and wall material further support the underlying physics for HDL, which originates from the extreme edge plasma region, like the SOL region.

Previously, the studies of the HDL in JET-ILW have distinguished the different operation phases, and how an increase of density affects plasma stored energy and confinement. It has successfully excluded excessive radiation, MARFE and divertor detachment as the causes of the H–L back transition. The aim of this work is to investigate the influence of the plasma edge physics parameters on the HDL and to provide a more complete experimental picture of this topic to help understand the underlying mechanism. The rest of the paper is organized as follows: the experimental method, including the development of a reliable estimator for the minimum of the radial electric (E_r) at the JET edge, is described in section 2. In section 3, the correlation between the ideal MHD parameter and separatrix density is analysed and the evolution of the edge E_r well during the different phases for HDL is surveyed. In section 4, the possible underlying physics mechanisms are discussed. Finally, section 5 presents a summary together with the implications for ITER and future burning plasma devices and future plans for this work.

2. Experimental methods and estimation of $E_{r,\,min}$

The high-resolution Thomson scattering (HRTS) diagnostic on JET simultaneously measures electron density (n_e) and electron temperature (T_e) profiles with up to 63 points along the outer radius of the plasma [17]. The system started reliable routine operation in 2007. More recently, the optical design of the laser input system and the instrument function has been improved to provide a resolution that enables the study of the plasma characteristics in the edge region [18].

In this paper, the simple line fit method described in [19] will be used to determine plasma pedestal parameters for JET plasma, as demonstrated in figure 1(*a*). Profiles in the SOL region in many devices are often found to exhibit a two-zone structure: a short gradient length scale region in density and temperature near the separatrix where most power exhaust occurs (near SOL), and a longer gradient length region further out (far SOL). On JET, the HRTS data at the lowest density, which covers the entire far SOL, is rather noisy and so is excluded from the analysis. Thus, the remaining measured HRTS SOL profile on JET includes only the near SOL short gradient length region, as shown in figure 1(*b*).

Based on the experimental observation that the profiles in the near SOL are nearly exponential, consistent with all the analysed discharges on AUG, the decay lengths in the near SOL region can be evaluated by a log-linear fit in the near SOL region, as introduced in [20]. In the previous studies [20, 21], although the analysis for the near SOL starts from the separatrix position (estimated as the point where $T_e = 100$ eV), the profile structure on both AUG and JET shows that the exponential decay starts from somewhere inside the separatrix. The Goldston HD model considers that the gradient scale lengths reach into the main plasma one gradient scale length, as that is the distance over which the grad-B drift 'smears' the edge [22]. The exponential nature of the profile in the near SOL means that the measured decay length does not vary much across the near SOL. The results with varying fit interval length across the separatrix on AUG have confirmed that the analysis is

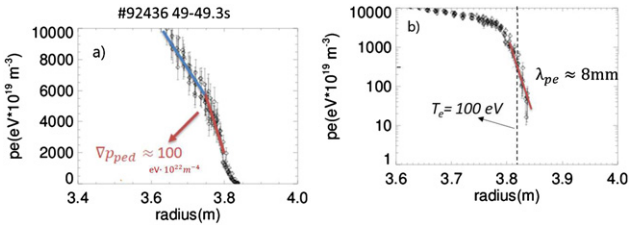

Figure 1. The electron pressure from HRTS measurements plotted against the JET major radius for an example JET discharge. (*a*) A linear-linear plot to illustrate how the pedestal gradient is estimated; (*b*) a log-linear fit to illustrate how the edge gradient decay length is estimated.

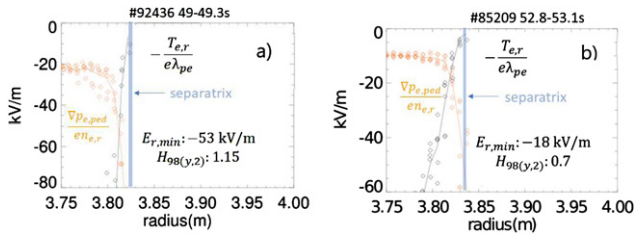

Figure 2. Demonstration of the method for estimating the edge radial electric field minimum, $E_{\mathrm{r,\,min}}$. Derived electric field against the JET major radius for (*a*) a typical H-mode with good confinement; (*b*) a high-density pulse with degrading confinement pulse.

relatively insensitive to the chosen position at the separatrix [23]. As can be seen in figure 1(*b*), the reliable data in the near SOL in JET-ILW are limited. To increase the reliability of the analysis, the decay lengths for the near SOL region are estimated by including the data inside the separatrix, as shown in figure 1(*b*).

Previous experimental studies [24–27] found that, for the main ion species, the pressure gradient term is the main contribution in the radial force balance and thus, E_{r} can be estimated by the gradient of main ion pressure, $E_{\mathrm{r}} \approx \nabla p_{\mathrm{i}}/en_{\mathrm{i}}$. This method is only valid for the confined region and estimation of E_{r} in the SOL region will be introduced in section 3.2. Following [11], for high density plasma, electron kinetic measurements from the TS system can be used to determine E_{r}, consistent with CXRS results. Since the Z_{eff} is rather low for JET-ILW, around 1.2–1.4 and it is reasonable to assume that $T_{\mathrm{i}} \approx T_{\mathrm{e}}$ and $n_{\mathrm{i}} \approx n_{\mathrm{e}}$ for high density JET pulses, thus, E_{r} can be estimated by $E_{\mathrm{r}} \approx \nabla p_{\mathrm{i}}/en_{\mathrm{i}} \approx \nabla p_{\mathrm{e}}/en_{\mathrm{e}}$, where all the parameters are routinely measured on JET-ILW. Although the principle is simple, it is still difficult to perform a reliable evaluation. The traditional way is to perform a curve fit to the kinetic profile and then calculate the gradient from the smooth curve. For the pedestal region, the variation of gradient is small, and it is rather easy to get reliable values. While it approaches the separatrix, the gradient changes dramatically, and the fast change of the gradient cannot be resolved on JET with the existing diagnostical resolution. Instead, a different approach will be introduced. As can be seen in figure 1(*a*), a simple line fit can be used to estimate the pedestal gradient (in red), while the estimated value is obviously only applicable for the region where $p_{\mathrm{e}} > 2000\,\mathrm{eV} \times 10^{19}\,\mathrm{m}^{-3}$. For the region across the separatrix, the exponential decay can describe the profile and a simple log-linear fit can be used to evaluate the gradient decay length and this is only applicable for the region where $p_{\mathrm{e}} < 2000\,\mathrm{eV} \times 10^{19}\,\mathrm{m}^{-3}$. For the region where $p_{\mathrm{e}} < 2000\,\mathrm{eV} \times 10^{19}\,\mathrm{m}^{-3}$, E_{r} can be estimated by an adapted form, $E_{\mathrm{r}} \approx \frac{\nabla p_{\mathrm{e}}}{en_{\mathrm{e,r}}} \approx \frac{1}{en_{\mathrm{e,r}}} \cdot \left(-\frac{p_{\mathrm{e}}}{\lambda_{p\mathrm{e}}}\right) = -\frac{T_{\mathrm{e,r}}}{e\lambda_{p\mathrm{e}}}$. The estimation of $E_{\mathrm{r,\,min}}$ for JET-ILW plasma with different plasma confinement is illustrated in figures 2(*a*) and (*b*). In the figures, the orange curves represent $\frac{\nabla p_{\mathrm{e}}}{en_{\mathrm{e,r}}}$ and the blue one $-\frac{T_{\mathrm{e,r}}}{e\lambda_{p\mathrm{e}}}$, the intersection gives a simple estimator for the minimum E_{r} of the electric field well at the edge, $E_{\mathrm{r,\,min}}$.

3. Experimental results

3.1. Correlation with ballooning stability at the separatrix

The experimental results from several tokamaks suggest that the edge plasma region, a zone that extends across the separatrix into the scrape-off layer (SOL), plays a key role in the observed the density limit for the high-performance plasma. In [22], it is proposed that the HDL may be caused by an MHD instability in the SOL close to the separatrix rather than originating in the core plasma or pedestal. In a recent study [15], the MHD-normalized pressure gradient at the separatrix, $\alpha_{\mathrm{MHD,sep}}$, in both AUG and JET is observed to rise linearly with the separatrix density normalized to the Greenwald value. The results from a dataset with a wide range of plasma parameters are consistent with earlier predictions based on the heuristic drift-based model. When $\alpha_{\mathrm{MHD,sep}}$ reaches ≈ 2.0–2.5, consistent with the theoretically predicted onset of ballooning modes, confinement degrades, and the density limit of the H-mode is found. In the more recent study [23], it is further concluded that the maximum achievable density on AUG without confinement degradation does appear to be given by the ideal ballooning limit. The dataset used included some type I ELMy pulses from JET with normalized separatrix density, $n_{\mathrm{e,sep}}/n_{\mathrm{GW}} < 0.4$. For this paper, a wider dataset has been compiled including many high density pulses from previous JET-ILW studies [12–14].

The ballooning parameter for the separatrix position, $\alpha_{\mathrm{MHD,sep}}$, can be expressed as:

$$\alpha_{\mathrm{MHD,sep}} = \frac{Rq_{95}^2 \nabla p_{\mathrm{sep}}}{B_{\mathrm{t}}^2/2\mu_0} = \frac{Rq_{95}^2}{B_{\mathrm{t}}^2/2\mu_0} \cdot \frac{2p_{\mathrm{e,sep}}}{\lambda_{p,\mathrm{SOL}}}.$$

Here, R is the plasma major radius, $\lambda_{p,\mathrm{SOL}}$ is the measured pressure decay length in the near SOL, B_{t} is the toroidal magnetic field, q_{95} is the safety factor on the plasma surface with 95% of the poloidal magnetic flux of the last closed flux surface (LCFS), and $p_{\mathrm{e,sep}}$ is the measured electron pressure. The temporal evolution of a typical high density H mode discharge in JET-ILW is illustrated in figure 1 of [12] and it be described by three main stages: a type I ELM phase, then a dithering H-mode phase with energy confinement deterioration, followed by the L-mode phase. As shown in figure 3, despite the different global parameters ($I_p = 1$–3 MA; $B_{\mathrm{t}} = 1.7$–3.4 T; $P_{\mathrm{tot}} =$

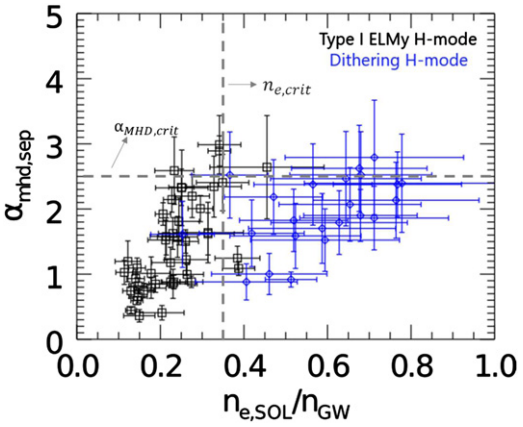

Figure 3. Ideal ballooning parameter, $\alpha_{\mathrm{MHD,sep}}$, against the separatrix electron density normalised to the Greenwald density limit, $n_{\mathrm{e,sep}}/n_{\mathrm{GW}}$, for the type I ELMy H-mode and dithering H-mode discharges in the JET-ILW dataset.

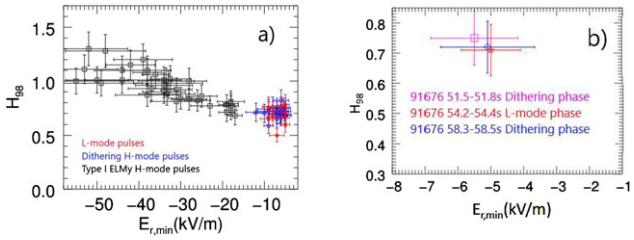

Figure 4. Normalized global energy confinement, $H_{98(y,2)}$, against minimum electric field inside the separatrix, $E_{\mathrm{r,\,min}}$, for (*a*) the full JET-ILW dataset; (*b*) for three phases of the single discharge #91676.

5–33 MW), the ballooning parameter increases almost linearly as normalized density at the separatrix until the $\alpha_{\mathrm{MHD,crit}} \approx 2.5$, when $n_{\mathrm{e,sep}}/n_{\mathrm{GW}} \approx 0.35$, which is consistent with the previous results on AUG. This is the case for most of the type I ELMy pulses. After the density reaches this critical value, the plasma confinement degrades and enters a dithering H-mode. The dithering H-mode phase can last up to 0.5 s, which enables a (≈20%) higher HDL than in JET-C. $n_{\mathrm{e,sep}}/n_{\mathrm{GW}}$ can reach up to 0.75 before the plasma enters the L-mode phase. In figure 3, the points from the dithering phase (in blue) are taken just before H–L back transition. $\alpha_{\mathrm{MHD,sep}}$ increases broadly linearly with $n_{\mathrm{e,sep}}$, until the normalized $n_{\mathrm{e,sep}}$ reaches a critical value, $n_{\mathrm{e,crit}} \approx 0.35$, corresponding to a critical $\alpha_{\mathrm{MHD,sep}} \approx 2.5$, as for AUG. Once $\alpha_{\mathrm{MHD,sep}}$ reaches the critical value, confinement degrades. The very large range of $n_{\mathrm{e,sep}}$ with $n_{\mathrm{e,sep}} > 0.35$ during the degradation phase on JET implies that the HDL is NOT directly set by ballooning stability at the separatrix. As shown in figure 3, for many pulses with $n_{\mathrm{e,sep}} > n_{\mathrm{e,crit}}$, $\alpha_{\mathrm{MHD,sep}}$ is well below the critical ballooning parameter, $\alpha_{\mathrm{MHD,crit}}$. Hence, for the JET high density pulses, reaching critical separatrix density and the corresponding critical ballooning parameter causes confinement degradation, as for AUG, but another mechanism must cause the H–L back transition and so set the HDL.

3.2. Role of the edge radial electric field for high density plasma

Turbulent transport can be largely suppressed by shear flows in fusion machine, particularly at the edge [28]. When a turbulent eddy is placed in a background flow, the gradient of flow velocity can tear the eddy apart leading to a reduction of the eddy correlation length and therefore of turbulent transport. The decorrelation of eddies takes places only when the background $E \times B$ velocity shear, $|\nabla V_{E\times B}| = \left|\frac{\nabla E_{\mathrm{r}}}{B}\right|$ is strong enough. $E \times B$ velocity shear is widely accepted to be responsible for the suppression of the edge turbulence, thus leading to the formation of the edge transport barrier (ETB) in H-mode plasma. The radial electric field is observed to exhibit negative E_{r} well with the minimum localized close to the separatrix and the $E_{\mathrm{r,\,min}}$ is found empirically a good proxy for the gradient of radial electric field [24, 25]. A critical $E_{\mathrm{r,\,min}}$ is observed to be required to access the H-mode. For AUG it is found to be around -15 kV m^{-1} [25, 29].

In this section, the role of $E_{\mathrm{r,\,min}}$ will be studied in type I ELMy H-mode, dithering H-mode prior to HDL and L-mode on JET-ILW to investigate the role of shear flow on different operational phases for HDL pulses on JET-ILW. As shown in figure 4(*a*), JET-ILW radial ETB wells are observed with $E_{\mathrm{r,\,min}}$ in the range -15 to -60 kV m^{-1} in high performance H-modes, consistent with previous CXRS results of AUG [25]. For the dithering H-mode phase prior to HDL, ETB well becomes shallower and $E_{\mathrm{r,\,min}}$ increases above -15 kV m^{-1}. In this phase, the normalised global plasma energy confinement, $H_{98(y,2)}$ [6, 30], degrades considerably to values of $H_{98(y,2)} \approx 0.75$. The degradation of confinement is obviously related to the decrease of $|E_{\mathrm{r,min}}|$, i.e. the decrease of E_{r} shear. However, the unexpected result is that $E_{\mathrm{r,\,min}}$ for the edge plasma well is observed to vary little between the L-mode and dithering phases, suggesting that the final back transition to L-mode phase is not due to a reduction of the inner negative shear of E_{r} well.

The result in figure 4(*b*) shows this also to be the case for a single discharge, #91676, which alternates from dithering phase to L-mode and back to dithering phase while input power and global plasma parameters remain relatively constant. This might suggest that the dithering phase is just in the same state as the L-mode phase. However, in the full dataset, although the pedestal gradient for the dithering phase is much shallower than that for type I ELMy H-mode, it is 2–3 times steeper than that for L-mode phase, as shown in figure 5(*a*). In #91676, n_{e} and T_{e} measured at the well minima are significantly higher for the dithering phase, as shown in figure 5(*b*). This implies that a small edge barrier is maintained during the dithering phase and, hence, there is indeed a bifurcation in the plasma state between the two phases.

The results of $E_{\mathrm{r,\,min}}$ show little difference between the dithering phase and L-mode phase. The electric field outside the separatrix is now considered. In the SOL region, plasma potential can be estimated as $V_{\mathrm{SOL,u}} \approx 3k\ T_{\mathrm{et}}/\mathrm{e} + 0.71k(T_{\mathrm{eu}} - T_{\mathrm{et}})/\mathrm{e}$ [31], and used to determine the peak SOL E-field, $E_{\mathrm{r,SOL}}$. Here in the equation, T_{eu} is the upstream separatrix temperature and T_{et} the divertor target temperature. In this paper, T_{eu} is estimated by assuming the separatrix is

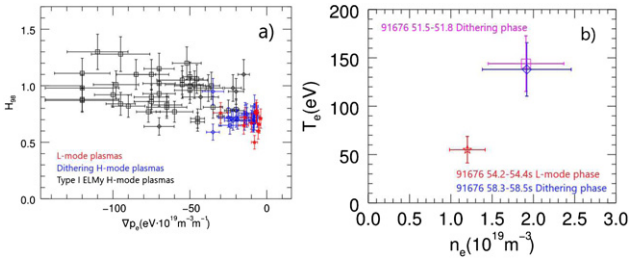

Figure 5. (*a*) Normalized global energy confinement, $H_{98(y,2)}$, against pedestal electron pressure gradient for the JET-ILW dataset of figure 4(*a*); (*b*) the edge electron temperature and edge electron density for the same discharge and phases as in figure 4(*b*).

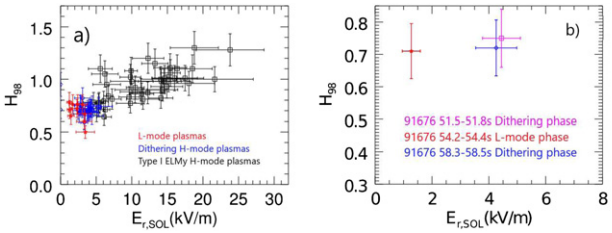

Figure 6. Normalized global energy confinement, $H_{98(y,2)}$, against radial electric field in the SOL, $E_{r,SOL}$, for (*a*) the JET-ILW dataset of figure 4(*a*); (*b*) the single discharge and phases of figure 4(*b*).

one decay length away from where the $E_{r,\,min}$ locates. Due to the lack of accurate measurements on the target temperature, T_{et} is evaluated by the two-point model form [31]: $T_t = \left[T_u^{7/2} - \frac{7}{2}\frac{\left(P_{SOL}/A_{q_\parallel}\right)L}{k_0}\right]^{2/7}$. Here, $L = \pi R q_{95}$ is the connection length and $A_{q_\parallel} = 4\pi R \lambda_q B_\theta / B_T$ is the surface area for the parallel power flux, B_θ is the poloidal magnetic field, and B_T is the toroidal magnetic field. $\lambda_q = \frac{2}{7}\lambda_{T_e,u}$ is used to calculate $A_{q_\parallel}$. For type I ELMy H-mode plasma, the trend of $E_{r,SOL}$ against confinement is similar with that of $E_{r,\,min}$, the confinement increases as the absolute value of $E_{r,SOL}$ increase. $E_{r,SOL}$ decreases in dithering H-mode phase, consistent with the degradation of confinement. However, compared with that in L-mode phase, $E_{r,SOL}$ is generally higher in the dithering phase, as can be seen in figure 6(*a*). Figure 6(*b*) shows that the difference is even clearer for the different phases of the single discharge #91676, which have similar plasma global parameters.

To further demonstrate how the E_r gradient evolves during the different phases, both $E_{r,\,min}$ and $E_{r,SOL}$ are plotted against the JET major radius in figure 7. The separatrix positions are taken to be located at the point where E_r goes to zero and indicated in the figure. Although the locations of $E_{r,\,min}$ seems unchanged within uncertainty, the distance to the separatrix position increases in L-mode phase due to the profile broadening. Both the lower $E_{r,SOL}$ and the more radially outward location of the peak due to pressure profile broadening combine to result in the smaller E_r gradient in the L-mode phase compared to the dithering or H-mode phases. The observed behaviour of $E_{r,\,min}$ and $E_{r,SOL}$ implies that the positive E_r shear gradient at the separatrix is higher in the dithering phase than

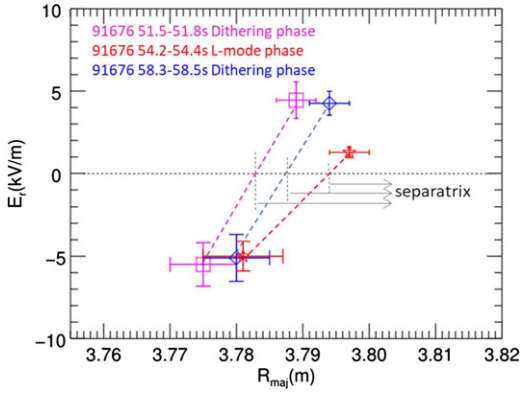

Figure 7. The radial electric field plotted against JET radius and the separatrix position, which is assumed to be located where E_r goes to zero.

in L-mode. The higher positive E_r gradient at the separatrix sustains a small ETB and enables access to higher density when compared to JET-C discharges that do not enter a dithering phase. The weakening of this positive E_r shear gradient eventually triggers the final H–L back transition.

4. Discussion of possible underlying physics mechanisms

The $E \times B$ velocity and its associated shear are believed to be responsible for the turbulence shear at the plasma edge and thus central to the physics of the transition between different plasma phases. As summarized in the review paper [32], any contribution to E_r can influence the transition between different phases. While it remains unclear which mechanism is the most important player in setting the fast transition, it is clear that the background flows driven by diamagnetic velocity are the fundamental player for locking in a steady state phase after the initial turbulence suppression/increase. In this paper, each phase is treated as steady state and the main contribution for E_r in the confined region is assumed to come from the diamagnetic term, $E_r \approx \frac{\nabla p_i}{e n_i}$, while the E_r in the SOL can be evaluated by calculating the upstream potential based on the two-point model [31]. While the H-mode confinement phase of the JET-ILW plasma has been shown to be compatible with high E_r shear at the ETB, the dithering phase of these plasmas has similar $E_{r,\,min}$ to L-modes. However, the broadening of pressure profiles in the SOL decreases and broadens the SOL E_r profile in the L-mode phase resulting in a flatter E_r profile across separatrix. It appears that, for the dithering phase, a barrier is sustained by a steeper positive E_r gradient across the separatrix. This result is consistent with the previous EDGE2D-EIRENE modelling that shows that E_r across the separatrix plays an important role in setting different H-mode power thresholds with different wall materials [33]. As density continues to increase, the turbulence increases and a further cooling down in the SOL and divertor region decreases the potential in the SOL region. Together with the increase of E_r relative distance to the separatrix, due to pressure profile broadening, the E_r positive gradient decreases and the barrier collapses and the plasma transits to L-mode.

The plasma state and turbulence character of the edge plasma on AUG [23] and C-mod [34] has been shown to be largely governed by two dimensionless parameters, α_{MHD} and normalized plasma collisionality, in agreement with the edge plasma stability phase-space proposed by Roger *et al* [35]. This two-parameter phase space can explain the edge plasma behaviour on JET-ILW as well. For low collisionality, the plasma is in the drift-wave regime and the turbulence can be largely suppressed if the $E \times B$ shear is large enough (corresponding to a threshold for $E_{\mathrm{r,\,min}}$). The plasma pressure gradient can increase as density increases until α_{MHD} reaches the ideal MHD stability limit when the plasma is in so-called stable H-mode phase. As collisionality increases, the plasma enters resistive regimes, the perpendicular transport is enhanced by resistive modes and the confinement degrades even when α_{MHD} is well below the limit of ideal ballooning instability. The enhanced transport reduces the pressure gradient and cools down the plasma and the shear of background flow decreases, corresponding to a decrease of $E_{\mathrm{r,\,min}}$. In this phase, the fluctuation level increases and the contribution from Reynolds stress drive may be non-negligible, and so the estimation of $E_{\mathrm{r,\,min}}$ from the diamagnetic velocity is likely to be underestimated. Simulation of turbulence with BOUT [36] shows that large perpendicular transport can be induced by resistive modes peaked in the SOL. The negative E_{r} inside the separatrix is generated by the Reynolds stress, and positive E_{r} in the far SOL is dominated by the sheath physics due to parallel particle loss. Near the separatrix in the SOL, the two mechanisms compete. As density increases and temperature decreases, the negative E_{r} inside the separatrix increases and enhances the Reynolds stress, while the positive E_{r} in the SOL reduces due to the decrease of sheath potential. The competition between the Reynolds stress drive and the sheath drive weakens the positive E_{r} shear layer, causing the final back transition to L-mode phase.

By adapting the normalized collisionality to a turbulence control parameter α_{t} [23], the AUG dataset shows that when approaching $\alpha_{\mathrm{t}} \approx 1$, a significant widening of pressure decay length is observed, consistent with previous findings [20] and generalized Heuristic drift model [37]. Across a dataset of JET-ILW L-mode, H-mode and dithering plasma, normalised SOL width is found to increase with increasing collisionality, figure 8, in agreement with previous observation on AUG. The operational phases for JET-ILW are generally similar with AUG and JET-C, except there are always dithering cycles during confinement degrading phase and before final back transition. On JET-ILW the density shows stronger oscillation during the dithering phase: a reduction after H–L transition and the increase of the density with the following L–H transition. On AUG, however, the density increases after the H–L transition. Thus, a hypothesis for the dithering H-mode phase for JET-ILW plasma close to HDL is proposed with a H–L–H–L- oscillations: as $n_{\mathrm{e,SOL}}$ is increased, the edge collisionality, $\nu_{*,\mathrm{SOL}}$, increases with it. The SOL broadens in line with the previously observed scaling. The broader SOL results in decreased E_{r} shear in the confined and the SOL regions. This process continues until the $E \times B$ shear is insufficient to maintain the ETB and a transition to L-mode occurs.

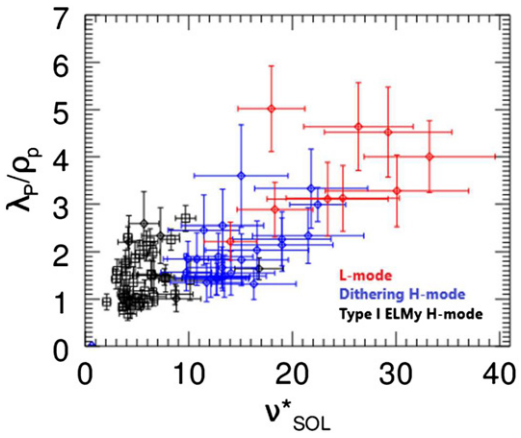

Figure 8. Normalised SOL width against SOL collisionality for the same set of JET-ILW plasma.

$n_{\mathrm{e,SOL}}$ decreases with the reduced confinement and the process repeats in reverse until $E \times B$ shear is sufficient to maintain an ETB and a transition to H-mode occurs.

However, what leads the difference between the density changes when it is close to the HDL is still unknown. One possible candidate is the low Z impurity content. Carbon content levels were reduced by a factor of 20 after the installation of JET ITER-like wall [38]. In contrast, the carbon concentrations only fell by 2–3 times on AUG when it moved from a C to a W wall. Whether the stronger density modulation caused by the ionized profiles in the edge plays a role in setting this dithering phase on JET-ILW can be tested with SOLPS-ITER in the future.

5. Summary

A study has been performed of a wide dataset of JET plasma with the Be/W ITER-like wall (JET-ILW) including H-mode plasmas where the edge density is raised until a transition to L-mode is observed. The results show that reaching the edge MHD ballooning limit leads to confinement degradation, as in previous studies of JET-C and AUG plasmas. However, unlike in AUG and JET-C, JET-ILW plasmas that exceed this limit enter a dithering phase associated with a higher a (≈20%) HDL than JET-C equivalents.

A new, reliable estimator of the minimum radial electric field in the ETB well, $E_{\mathrm{r,\,min}}$, for JET has been derived by combining HRTS measures of pedestal gradient and edge-SOL decay lengths. For high performance JET-ILW H-modes, $E_{\mathrm{r,\,min}}$ are observed in the range -15 to -60 kV m^{-1} consistent with previous CXRS results in AUG. $E_{\mathrm{r,\,min}}$ is found to be similar for JET-ILW dithering and L-mode despite the fact that the dithering phase has considerably (2–3 times) higher $n_{\mathrm{e,ped}}$ and $T_{\mathrm{e,ped}}$. Due to the broadening of the plasma pressure profile, the relative distance of $E_{\mathrm{r,\,min}}$ to the separatrix position increases in L-mode phase. In addition, $E_{\mathrm{r,SOL}}$ is found to be 2–3 times higher in the dithering phase than in L-mode. Taken together, these results imply that the dithering phase has significantly higher E_{r} shear in the positive shear region around the LCFS than the L-mode. This higher shear could play a role in sustaining a marginal phase in JET-ILW, thus a higher HDL

than that in JET-C. The results are consistent with the generalized HD (GHD) model [37] and recent BOUT++ simulation results [39], in which it was found that the $E \times B$ shearing rate in the SOL plays the dominating role for sustaining H-mode plasma.

The results of the JET-ILW dataset show agreement with previous AUG observation and the GHD model for SOL broadening at high collisionality. A hypothesis for the dithering H-mode phase observed in JET-ILW plasma is proposed with a cycle of H–L and L–H transitions with a mechanism that can be summarised as:

- n_e increases $\rightarrow \nu_{*,SOL}$ increases $\rightarrow$ SOL broadens $\rightarrow$ E_r shear decreases $\rightarrow$ H–L transition;
- n_e decreases $\rightarrow$ $\nu_{*,SOL}$ decreases $\rightarrow$ SOL narrows $\rightarrow$ E_r shear increases $\rightarrow$ L–H transition.

The different behaviour between JET-ILW and JET-C plasma remains unexplained but may be due to different low-Z ion concentrations of the plasma.

The results suggest that ITER could be operated in H-mode with higher density, but likely with a dithering phase plasma with lower confinement. For ITER, and other burning plasma devices, operating just below the MHD limit for the dithering phase could be a promising regime for maximising core density and fusion performance while minimising plasma-material interaction. The oscillatory signal during the dithering phase could be used as a precursor of undesirable plasma performance for control purposes.

Acknowledgments

This work has been carried out within the framework of the EUROfusion Consortium and has received funding from the Euratom research and training programme 2014–2018 and 2019–2020 under Grant Agreement No. 633053 and from the RCUK (Grant No. EP/T012250/1). To obtain further information on the data and models underlying this paper please contact. The views and opinions expressed herein do not necessarily reflect those of the European Commission. This work was also performed under the US. Department of Energy by Lawrence Livermore National Laboratory under Contract No. DE-AC52-07NA27344, and by PPPL under Contract No. DE-AC02-09CHII466.

ORCID iDs

H.J. Sun https://orcid.org/0000-0003-0880-0013
R.J. Goldston https://orcid.org/0000-0002-0368-5514
A. Huber https://orcid.org/0000-0002-3558-8129
J.R. Harrison https://orcid.org/0000-0003-2906-5097
F. Militello https://orcid.org/0000-0002-8034-4756

References

[1] Gormezano C. *et al* 2007 Chapter 6: steady state operation *Nucl. Fusion* **47** S285–336
[2] Loarte A. *et al* 2007 Chapter 4: power and particle control *Nucl. Fusion* **47** S203–63
[3] Greenwald M., Terry J.L., Wolfe S.M., Ejima S., Bell M.G., Kaye S.M. and Neilson G.H. 1988 *Nucl. Fusion* **28** 2199
[4] Greenwald M. 2002 *Plasma Phys. Control. Fusion* **44** R27–53
[5] Mertens V. *et al* 1997 *Nucl. Fusion* **37** 1607
[6] ITER Physics Expert Group on Confin Transport, ITER Physics Expert Group on Confin Database and ITER Physics Basis Editors 1999 Chapter 2: plasma confinement and transport *Nucl. Fusion* **39** 2175–249
[7] Doyle E.J. *et al* 2007 Chapter 2: plasma confinement and transport *Nucl. Fusion* **47** S18–S127
[8] Borrass K. *et al* 2004 *Nucl. Fusion* **44** 752–60
[9] Mertens V., Borrass K., Gafert J., Laux M. and Schweinzer J. (ASDEX Upgrade Team) 2000 *Nucl. Fusion* **40** 1839
[10] Maingi R. *et al* 1997 *Phys. Plasmas* **4** 1752
[11] Bernert M. *et al* 2015 *Plasma Phys. Control. Fusion* **57** 014038
[12] Huber A. *et al* 2017 *Nucl. Fusion* **57** 086007
[13] Huber A. *et al* 2013 *J. Nucl. Mater.* **438** S139–49
[14] Huber A. *et al* 2015 *J. Nucl. Mater.* **463** 445–9
[15] Eich T., Goldston R.J., Kallenbach A., Sieglin B. and Sun H.J. 2018 *Nucl. Fusion* **58** 034001
[16] Lipschultz B., LaBombard B., Marmar E.S., Pickrell M.M., Terry J.L., Watterson R. and Wolfe S.M. 1984 *Nucl. Fusion* **24** 977
[17] Pasqualotto R., Nielsen P., Gowers C., Beurskens M., Kempenaars M., Carlstrom T. and Johnson D. 2004 *Rev. Sci. Instrum.* **75** 3891
[18] Frassinetti L., Beurskens M.N.A., Scannell R., Osborne T.H., Flanagan J., Kempenaars M., Maslov M., Pasqualotto R. and Walsh M. 2012 *Rev. Sci. Instrum.* **83** 013506
[19] Schneider P.A. *et al* 2012 *Plasma Phys. Control. Fusion* **54** 105009
[20] Sun H.J., Wolfrum E., Eich T., Kurzan B., Potzel S. and Stroth U. 2015 *Plasma Phys. Control. Fusion* **57** 125011
[21] Sun H.J. *et al* 2017 *Plasma Phys. Control. Fusion* **59** 105010
[22] Goldston R.J. 2012 *Nucl. Fusion* **52** 013009
[23] Eich T., Manz P., Goldston R.J., Hennequin P., David P., Faitsch M., Kurzan B., Sieglin B. and Wolfrum E. 2020 *Nucl. Fusion* **60** 056016
[24] McDermott R.M. *et al* 2009 *Phys. Plasmas* **16** 056103
[25] Viezzer E. *et al* 2013 *Nucl. Fusion* **53** 053005
[26] Maggi C.F. *et al* 2014 *Nucl. Fusion* **54** 023007
[27] Ryter F. *et al* 2016 *Plasma Phys. Control. Fusion* **58** 014007
[28] Biglari H., Diamond H. and Terry P.W. 1990 *Phys. Fluids* B **2** 1
[29] Sauter P., Pütterich T., Viezzer E., Wolfrum E., Conway G.D., Fischer R., Kurzan B., McDermott R.M. and Rathgeber S.K. 2012 *Nucl. Fusion* **52** 012001
[30] McDonald D.C. *et al* 2007 *Nucl. Fusion* **47** 147
[31] Stangeby P.C. 2000 *The Plasma Boundary of Magnetic Fusion Devices* (Bristol: Institute of Physics Publishing)
[32] Connor J.W. and Wilson H.R. 2000 *Plasma Phys. Control. Fusion* **42** R1–R74
[33] Chankin A.V., Delabie E., Corrigan G., Harting D., Maggi C.F. and Meyer H. 2017 *Plasma Phys. Control. Fusion* **59** 045012
[34] LaBombard B., Hughes J.W., Mossessian D., Greenwald M., Lipschultz B. and Terry J.L. (the Alcator C-Mod Team) 2005 *Nucl. Fusion* **45** 1658–75
[35] Roger B.N., Drake J.F. and Zeiler A. 1998 *Phys. Rev. Lett.* **81** 4396–9
[36] Xu X.Q., Nevins W.M., Rognlien T.D., Bulmer R.H., Greenwald M., Mahdavi A., Pearlstein L.D. and Snyder P. 2003 *Phys. Plasmas* **10** 1773–81
[37] Goldston R.J. and Eich T. 2019 Generalization of the heuristic drift model of the scrape off layer for finite *46th EPS Conf. on Plasma Physics* (Milan, Italy)
[38] Matthews G.F. 2013 *J. Nucl. Mater.* **438** S2–S10
[39] Li N.M., Xu X.Q., Goldston R.J., Sun J.Z. and Wang D.Z. 2021 *Nucl. Fusion* **61** 026005